

## Unified Band-Crossing Interpretation of $^{16}\text{O}+^{16}\text{O}$ Inelastic Reactions

K. Langanke, H. Friedrich, and S. E. Koonin

*W. K. Kellogg Radiation Laboratory, California Institute of Technology, Pasadena, California 91125*

(Received 18 March 1983)

A band-crossing model based on a microscopically derived  $^{16}\text{O}+^{16}\text{O}$  potential and the Pauli principle is used to interpret data on  $^{16}\text{O}+^{16}\text{O}$  reactions to eight inelastic channels. Structures observed in the cross sections are accounted for in all cases.

PACS numbers: 25.70.-z, 24.10.Eq, 27.30.+t

Cross sections for inelastic  $^{16}\text{O}+^{16}\text{O}$  scattering above  $E_{c.m.} \approx 15$  MeV show gross structure which has been interpreted in individual cases as due to the coupling between nearly degenerate resonances in the entrance channel and in the exit channel (double-resonance mechanism).<sup>1</sup> In the band-crossing model (BCM)<sup>2</sup> this idea has been reformulated with the assumption that the resonances in the elastic and inelastic channels form a single type of rotating dinuclear complex (molecular band). This model predicts a coupling of two channels whenever the respective bands in these channels cross. Although this picture has great physical appeal, some problems arise in practice. For example, in the BCM picture of Kondo, Bromley, and Abe<sup>3</sup> the elastic  $^{16}\text{O}+^{16}\text{O}$  channel couples to the inelastic  $3^-$  channels in the region  $22 \text{ MeV} \lesssim E_{c.m.} \lesssim 40 \text{ MeV}$ , while the experimental cross sections show structure for  $E_{c.m.} \gtrsim 15 \text{ MeV}$ . In addition, the observed structure in the strongly  $l$ -mismatched  $0_2^+$  and  $2^-$  channels definitely cannot be accounted for, as the respective bands do not even come close to each other in the relevant energy range.

In the present Letter, we interpret recent experimental data on  $^{16}\text{O}+^{16}\text{O}$  reactions to various inelastic channels in terms of a unified band-crossing model which is well founded microscopically. Microscopic considerations are important because the basic ingredient in the BCM of Ref. 3 is a *single* molecular band generated by the channel-independent  $^{16}\text{O}+^{16}\text{O}$  optical potential. However, accurate microscopic studies of elastic  $^{16}\text{O}+^{16}\text{O}$  scattering based on a variety of internucleon forces, e.g., in the framework of the generator-coordinate method (GCM), *invariably* lead to *two or more* rotational bands.<sup>4,5</sup> As we demonstrate below, the presence of such multiple bands is an important element in a simple interpretation of the data.

To interpret inelastic reactions in terms of a band-crossing picture we need the energies of the resonances in each channel. For elastic scattering, the results of such microscopic cal-

culations can be reproduced quite accurately with a local  $^{16}\text{O}+^{16}\text{O}$  potential,  $V(r)$ , if the radial dependence is chosen appropriately and if the wave function of relative motion,  $g_l(r)$ , is required to be orthogonal to a set of Pauli-forbidden states.<sup>6,7</sup> That is,  $g_l(r)$  satisfies the Schrödinger-like equation

$$\Lambda \left( -\frac{\hbar^2}{2M} \frac{d^2}{dr^2} + V(r) + \frac{l(l+1)\hbar^2}{2Mr^2} - E \right) g_l(r) = 0, \quad (1)$$

where  $M$  is the reduced mass,  $E$  the center-of-mass energy, and  $l$  the orbital angular momentum. The operator  $\Lambda$  is a projector ensuring that  $g$  does not lead to many-body states which violate the Pauli principle. If, as we assume, the internal states of the nuclei are described by the harmonic-oscillator shell model, then  $\Lambda$  projects off of all harmonic-oscillator states of relative motion with total quantum number  $2n+l < N_0=24$ , the "redundancy limit"<sup>7</sup>; here  $n$  is the radial quantum number of relative motion. The main effect of the orthogonality condition is to damp the wave function of relative motion inside a range which depends on the orbital angular momentum  $l$  and is roughly 4 fm for small  $l$  values.

When this "orthogonality-condition" description is extended to inelastic  $^{16}\text{O}+^{16}\text{O}$  channels, the structure of  $\Lambda$  will change, depending upon the excited states involved. If these internal excitations are described by the harmonic-oscillator shell model, then this change amounts to a decrease in the redundancy limit  $N_0$ . For each inelastic excitation, we have identified the shell-model configurations expected to dominate (one-particle, one-hole for the  $1^-$ ,  $2^-$ , and  $3^-$  states in  $^{16}\text{O}$  and two-particle, two-hole for the  $0^+$  and  $2^+$  states), and have modified the  $N_0$  values in each channel accordingly. For lack of more detailed information, we assume that the potential  $V$  is channel independent and equal to that determined from GCM calculations of elastic scattering.<sup>7</sup>

The basis of the present study is a set of bands of rotational states (Fig. 1). These appear as resonances in the scattering phase shifts, which are obtained by solving the equation of relative motion (1).<sup>4,7</sup> For each redundancy limit  $N_0$ , there are (at least) two rotational bands. Note that  $N_0$  (smallest allowed value of  $2n+l$ ) is even for even  $l$  and is odd for odd  $l$ . Since there are only positive-parity states in the initial elastic channel, resonances in the inelastic channels which can couple to elastic resonances will have odd  $l$  if the total internal parity of the  $^{16}\text{O}$  nuclei is odd.

A remarkable feature of our bands is the strong parity splitting between bands belonging to successive redundancy limits. This parity splitting is primarily the result of the greater range of the Pauli projector  $\Lambda$  in the odd partial waves, which is more pronounced for small  $l$ .<sup>8</sup> In contrast, the even bands corresponding to  $N_0 = 24, 22,$  and  $20$  are very similar. This  $N_0$  independence is also true for the odd-parity states corresponding to  $N_0 = 19, 21, 23,$  and  $25$ . Thus, the subsequent discussion is virtually independent of the precise value of  $N_0$  assigned to each inelastic channel, so long as the parity is chosen correct-

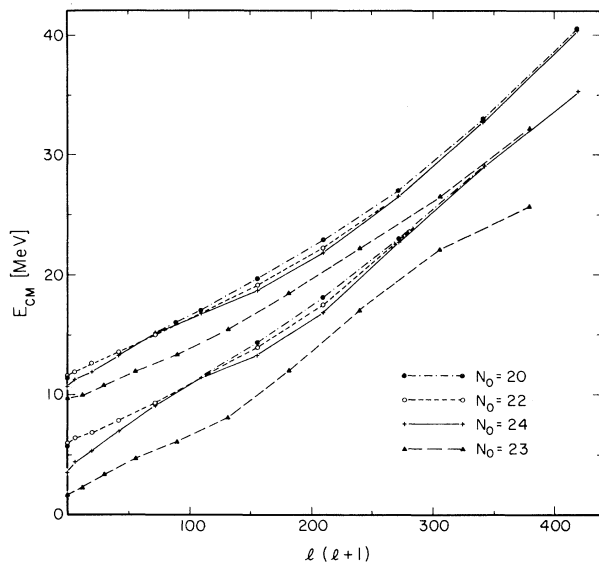


FIG. 1. Band structure in  $^{16}\text{O} + ^{16}\text{O}$  obtained by solving the equation of relative motion for the four-Gaussian effective potential of Ref. 7 and with  $N_0$  set to 24 (solid lines), 23 (short-dashed lines), 22 (long-dashed lines), and 20 (dash-dotted lines). Bands of lower-lying bound and quasibound states (widths  $\ll 1$  keV) have been omitted, because they are not expected to be manifest in the present experimental data.

ly. For each even  $N_0$  (positive parity) the upper band consists of rather broad "shape resonances" above the interaction barrier, while the lower band consists of longer-lived "molecular states." For odd  $N_0$  (negative parity) both bands are of the molecular type; the shape resonances are too broad to influence the cross section significantly.

We now interpret recent data on inelastic  $^{16}\text{O} + ^{16}\text{O}$  reactions<sup>9-11</sup> using band-crossing diagrams (Fig. 2) which are derived from Fig. 1 by assuming that the total angular momentum  $J$  is the sum of  $l$  and the channel spin  $I$  and that coupling to other channels does not shift the energies of the states. Recent experiments have shown that the aligned bands constructed in this way play the dominant role in the energy range under investigation.<sup>12</sup> Such a discussion of band-crossing diagrams has been shown to reveal the essential

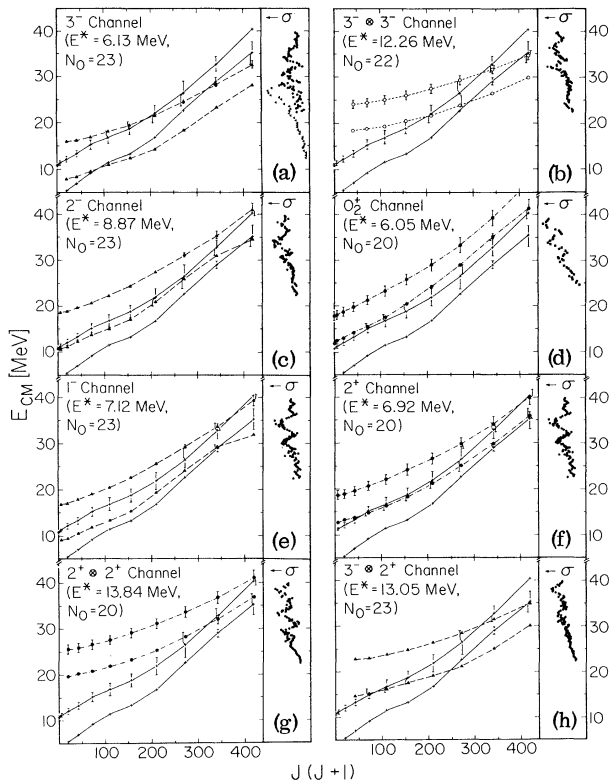


FIG. 2.  $^{16}\text{O} + ^{16}\text{O}$  band-crossing diagrams for various inelastic channels obtained as described in the text. The value of  $N_0$  adopted for each channel is shown. The bars show the calculated widths of the states. In the panels showing experimental data ( $\sigma$ ), (b), (c), (e)-(h) are inelastic excitation functions from Ref. 9, (a) is the  $\gamma$ -radiation deexcitation data of Ref. 10, and (d) the data of Ref. 11.

features emerging from a more complete study based on solving the corresponding coupled-channel equations.<sup>3</sup>

*The  $3^-$  channel.*—The band-crossing diagram predicts coupling in the energy region  $E_{c.m.} \approx 18$ –37 MeV, which is in excellent agreement with experiment. Moreover, the predicted energy regions of strong coupling are correlated with peaks in the experimental cross sections.<sup>10</sup> For  $E_{c.m.} \lesssim 27$  MeV shape resonances in the elastic channel couple with molecular states in the inelastic channel, while for  $E_{c.m.} \approx 27$ –37 MeV, the coupling is between two molecular states of comparable width. This latter coupling should be stronger than that below 27 MeV, because the states involved have greater overlap at relatively smaller distances. In fact, the experimental cross sections do show a marked rise near this energy. Note that without the parity splitting in the resonant structure our band-crossing diagram would not agree with the experimental data.

*The  $3^- \otimes 3^-$  channel.*—In agreement with the data, coupling is expected in the energy range  $E_{c.m.} \gtrsim 30$  MeV. The molecular band in the inelastic channel crosses the elastic bands near 22 and 24 MeV, but it may be too speculative to connect this crossing with the experimental structure near 24 MeV.

*The  $2^-$  channel.*—The band-crossing diagram predicts that the elastic-channel molecular resonance band couples to the lower inelastic molecular band for  $E_{c.m.} \approx 34$  MeV. At  $E_{c.m.} \approx 31$  MeV the elastic shape resonance overlaps with the inelastic-channel resonance of the lower molecular band whose width is  $\approx 2$  keV. Both of these energies correspond to structures in the data. At smaller energies the lower molecular states in the  $2^-$  channel are extremely narrow ( $\ll 1$  keV) and this may be the reason why no structures are seen in the data, although the resonances do overlap with elastic-channel shape resonances.

*The  $0_2^+$  channel.*—The coupling of the excited  $0^+$  channel to the elastic channel cannot be understood in the BCM of Ref. 3. In our analysis the coupling between the two channels is based on the coexistence of the molecular and shape resonances. Experimental data<sup>11</sup> available for  $E_{c.m.} \gtrsim 25$  MeV show broad structure around 30, 34, and 39 MeV; the band-crossing diagram predicts coupling of the shape resonances in the elastic channel to the molecular band at roughly these energies.

*The 7-MeV ( $1^-$ ,  $2^+$ ) channels.*—The band-crossing diagram predicts a coupling of the  $2^+$  channel

to the elastic channel for energies  $E_{c.m.} \gtrsim 14$  MeV, while the  $1^-$  channel should couple for energies above  $\approx 29$  MeV. This suggests that the experimental data at lower energies are dominated by the  $2^+$  channel.

*The  $2^+ \otimes 2^+$  channel.*—Coupling is predicted for energies  $E_{c.m.} \gtrsim 28$  MeV in agreement with experiment.

*The  $3^- \otimes 2^+$  channel.*—In the energy range investigated experimentally, our model predicts coupling of this channel to the elastic channel for  $E_{c.m.} \gtrsim 29$  MeV, again in agreement with experiment.

In addition to describing inelastic scattering, our band structure gives a possible explanation for the resonant structures found in the elastic and  $\alpha + {}^{28}\text{Si}$  reaction channels, for which the BCM approach of Ref. 3 cannot account. The narrow resonant structure with spins  $l=2$ –8 found for  $9.7 \text{ MeV} \lesssim E_{c.m.} \lesssim 12 \text{ MeV}$ <sup>13</sup> may be due to an excitation of the molecular states in an inelastic channel; e.g., the aligned states in the  $1^-$  channel reproduce these energies fairly well. Moreover, the narrow resonant structures with spin assignments  $J=8^+$  and  $J=10^+$  found in the reaction  ${}^{16}\text{O}({}^{16}\text{O}, \alpha){}^{28}\text{Si}$  near 16 MeV<sup>14</sup> can be understood via a two-step process in which the  $l=8$  or  $l=10$  shape resonance in the elastic channel excites an intermediate molecular state in an inelastic channel, which couples strongly to the  $\alpha + {}^{28}\text{Si}$  channel.<sup>15</sup>

We have presented a unified analysis of inelastic  ${}^{16}\text{O} + {}^{16}\text{O}$  scattering based on a band-crossing picture. The input was a microscopically derived  ${}^{16}\text{O} + {}^{16}\text{O}$  potential and the requirements of the Pauli principle. There are no adjustable parameters. In contrast to the usual optical-model approach this leads to coexisting shape and molecular resonances and a strong parity splitting of the bands. In the present case of inelastic  ${}^{16}\text{O} + {}^{16}\text{O}$  reactions the structure expected as a result of the coupling of bands in the elastic and various inelastic channels agrees well with experimental data. This agreement should serve to motivate further experimental studies to verify band coexistence (including other systems, such as the  ${}^{12}\text{C} + {}^{12}\text{C}$  case discussed by Langanke and Koonin<sup>16</sup>) and further theoretical calculations to verify our assumptions about the resonances in inelastic  ${}^{16}\text{O} + {}^{16}\text{O}$  channels.

This work was supported in part by the National Science Foundation through Grants No. PHY79-23638 and No. PHY82-07332 and by the Deutsche Forschungsgemeinschaft. We are grateful to P.

Paul and his colleagues for providing us with data prior to publication.

---

<sup>1</sup>B. Imanishi, Nucl. Phys. A125, 33 (1968); W. Scheid, W. Greiner, and W. Lemmer, Phys. Rev. Lett. 25, 176 (1970).

<sup>2</sup>Y. Kondo, Y. Abe, and T. Matsuse, Phys. Rev. C 19, 1356 (1979); Y. Abe, T. Matsuse, and Y. Kondo, Phys. Rev. C 19, 1365 (1979).

<sup>3</sup>Y. Kondo, D. A. Bromley, and Y. Abe, Prog. Theor. Phys. 63, 722 (1980), and Phys. Rev. C 22, 1068 (1980).

<sup>4</sup>H. Friedrich, Nucl. Phys. A224, 537 (1974); A. Tohsaki, F. Tanabe, and R. Tamagaki, Prog. Theor. Phys. 53, 1022 (1975); L. F. Canto, Nucl. Phys. A279, 85 (1977).

<sup>5</sup>K. Langanke, R. Stademann, and W. Timm, Phys. Rev. C 24, 1023 (1981).

<sup>6</sup>S. Saito, Prog. Theor. Phys. 41, 705 (1969).

<sup>7</sup>H. Friedrich and L. F. Canto, Nucl. Phys. A291, 249

(1977).

<sup>8</sup>H. Friedrich, Phys. Rep. 74, 209 (1981); H. Friedrich and K. Langanke, Phys. Rev. C (to be published).

<sup>9</sup>D. Abriola, J. S. Karp, R. L. McGrath, P. Paul, W. A. Watson, and S. Y. Zhiu, to be published.

<sup>10</sup>J. J. Kolata, R. C. Fuller, R. M. Freeman, F. Haas, B. Heusch, and A. Gallmann, Phys. Rev. C 16, 891 (1977), and 19, 2237 (1979).

<sup>11</sup>W. S. Freeman, H. W. Wilschut, T. Chapuran, W. F. Piel, and P. Paul, Phys. Rev. Lett. 45, 1479 (1980).

<sup>12</sup>W. Trautmann, to be published.

<sup>13</sup>G. Gaul, W. Bickel, W. Lahmer, and R. Santo, in *Resonances in Heavy Ion Reactions*, edited by K. A. Eberhard, Lecture Notes in Physics Vol. 156 (Springer-Verlag, Berlin, 1982), p. 72.

<sup>14</sup>M. Gai, E. C. Schloemer, J. E. Freedman, A. C. Hayes, S. K. Korotky, J. M. Manoyan, B. Shivakumar, S. M. Sterbenz, H. Voit, S. J. Willett, and D. A. Bromley, Phys. Rev. Lett. 47, 1878 (1981).

<sup>15</sup>K. Langanke, R. Stademann, and A. Weiguny, to be published.

<sup>16</sup>K. Langanke and S. E. Koonin, Phys. Lett. 123B, 21 (1983).